

Analytical Solution of the O-X Mode Conversion Problem

Francesco Volpe

*Dept of Engineering Physics, University of Wisconsin,
Madison, WI 53706, U.S.A.*

Abstract

The excitation of a slow extraordinary wave in a overdense plasma from an ordinary wave impinging on the critical layer in the plane spanned by the density gradient and magnetic field is solved analytically by formulating the problem in terms of a parabolic cylinder equation. A formula for the angular dependence of the transmission coefficient is derived.

Key words: magnetized plasmas, mode coupling

PACS: 52.35.Hr, 52.35.Mw

The mode conversion of an ordinary (O) into a slow extraordinary (SX) wave, first observed in ionospheric plasmas [1], has lately received great attention as part of the OXB process [2], where B denotes the electron Bernstein mode. This has been used with success for heating [3], temperature diagnostic [4] and current drive [5] of the W7-AS stellarator and other hot overdense magnetically confined laboratory plasmas [6,7].

The O-SX mode conversion has been solved in the past under the Wentzel-Kramers-Brillouin (WKB) approximation in one dimension (1D) [1,2,8,9,10], in 1D in presence of a sheared magnetic field [11], in two dimensions (2D) [12,13,14] and in 2D in presence of a sheared field [15]. Later it was the object of a numerical study [16].

The present Letter provides the first *analytical, non-WKB*-approximated solution of the problem. At the cost of a simpler geometry compared with Refs.[11,12,13,14,15], it leads to a relatively simple formula which allows to *visualize* the spatial dependence (Figs.4 and 6) and time evolution (Fig.5) of the wave as it tunnels through the O-SX evanescent layer. This might replace time-consuming *numerical* models in the interpretation of direct, space- and time-resolved measurements of the electric and magnetic field in the mode-conversion region [17].

Email address: fvolpe@wisc.edu (Francesco Volpe).

Consider a plasma magnetized along z and plane-stratified along x . Suppose the inhomogeneity to be weak enough to use the *local* dielectric tensor.

From the Vlasov-Maxwell system it follows, in the zero temperature limit, that

$$\nabla \times (\nabla \times \mathbf{E}) = \frac{\omega^2}{c^2} \epsilon \mathbf{E}, \quad (1)$$

where ϵ is the dielectric tensor for a cold magnetized plasma [18],

$$\epsilon = \begin{pmatrix} 1 - \frac{X}{1-Y^2} & -i \frac{XY}{1-Y^2} & 0 \\ i \frac{XY}{1-Y^2} & 1 - \frac{X}{1-Y^2} & 0 \\ 0 & 0 & 1 - X \end{pmatrix}, \quad (2)$$

$X = \omega_{pe}^2/\omega^2$ and $Y = \omega_{ce}/\omega$ are the dimensionless density and magnetic field, ω_{pe} and ω_{ce} the plasma and electron cyclotron angular frequency. We seek solutions of wave equation 1 in the form:

$$\mathbf{E}(x, y, z, \omega) = \mathbf{E}_0(x, \omega) e^{ik_z z}, \quad (3)$$

where the wavenumber k_z is real-valued. Note that this is not an eikonal ansatz and that no assumption is made on the dependence of \mathbf{E}_0 on x . Note also, however, that $k_y=0$, i.e. that the wave is assumed to propagate in the plane spanned by the density gradient ∇n (direction x) and by the magnetic field (parallel to z).

With this substitution, Eq.1 rewrites:

$$-\frac{\partial^2}{\partial x^2} \begin{pmatrix} 0 \\ E_{0y} \\ E_{0z} \end{pmatrix} + iN_z \frac{\omega}{c} \frac{\partial}{\partial x} \begin{pmatrix} E_{0z} \\ 0 \\ E_{0x} \end{pmatrix} = \frac{\omega^2}{c^2} \begin{pmatrix} 1 - \frac{X}{1-Y^2} - N_z^2 & -i \frac{XY}{1-Y^2} & 0 \\ i \frac{XY}{1-Y^2} & 1 - \frac{X}{1-Y^2} - N_z^2 & 0 \\ 0 & 0 & 1 - X \end{pmatrix} \begin{pmatrix} E_{0x} \\ E_{0y} \\ E_{0z} \end{pmatrix} \quad (4)$$

where $\mathbf{N} = c\mathbf{k}/\omega$ is the refractive index. In the remainder, x will be renormalized to the vacuum wavelength by replacing

$$x\omega/c \longrightarrow x, \quad (5)$$

Circular components $E_{0\pm} = (E_{0x} \pm iE_{0y})/\sqrt{2}$ permit to diagonalize the tensor on the right hand side:

$$-\frac{\partial^2}{\partial x^2} \begin{pmatrix} \frac{E_{0+}-E_{0-}}{2} \\ \frac{-E_{0+}+E_{0-}}{2} \\ E_{0z} \end{pmatrix} + i \frac{N_z}{\sqrt{2}} \frac{\partial}{\partial x} \begin{pmatrix} E_{0z} \\ E_{0z} \\ E_{0+} + E_{0-} \end{pmatrix} = \begin{pmatrix} \frac{X_L-X}{1+Y} & 0 & 0 \\ 0 & \frac{X_R-X}{1-Y} & 0 \\ 0 & 0 & X_P - X \end{pmatrix} \begin{pmatrix} E_{0+} \\ E_{0-} \\ E_{0z} \end{pmatrix} \quad (6)$$

The circularly polarized X-modes and the linearly, parallel to z polarized O-mode are indeed the *independent* eigensolutions of the *homogeneous* problem.

The derivatives on the left hand side introduce a medium *inhomogeneity* and, being *off-diagonal*, they *couple* the otherwise independent modes, accounting for their *conversions*.

The diagonal elements of Eq.6 have been expressed in terms of the cutoff densities

$$X_R = (1 - N_z^2)(1 - Y) \quad (7a)$$

$$X_L = (1 - N_z^2)(1 + Y) \quad (7b)$$

$$X_P = 1, \quad (7c)$$

These correspond to different parts of the cold dielectric tensor (R , L or P , in Stix notation [18]) being set to 0.

X_R is the cut-off for the “fast” (in the sense of the phase velocity) right-handed (R) X-mode. X_L and X_P , instead (Eqs.7b-c), are the slow X- and O-mode cutoff densities, X_{SX} and X_O respectively:

$$X_{SX} = X_L \quad (8a)$$

$$X_O = X_P \quad (8b)$$

if $N_z < N_{z,opt}$. If instead, $N_z > N_{z,opt}$,

$$X_O = X_L \quad (9a)$$

$$X_{SX} = X_P \quad (9b)$$

Here

$$N_{z,opt}^2 = \frac{Y}{Y + 1}, \quad (10)$$

is an optimal value of N_z^2 making the O- and slow X-mode degenerate. $N_{z,opt}$ is the optimal value of N_z yielding complete OX mode conversion [1,2,8,9].

From Eqs.7-10 it can be shown that X_O is always the smallest between X_L and X_P .

At $X \gg X_R$, where no fast X-mode exists ($E_- = 0$) we can restrict our attention to:

$$\left(\frac{X_L - X}{1 + Y} + \frac{1}{L_n^2} \frac{\partial_X^2}{2} \right) E_+ = i \frac{N_z}{L_n} \frac{\partial_X}{\sqrt{2}} E_z \quad (11a)$$

$$\left(X_P - X + \frac{1}{L_n^2} \partial_X^2 \right) E_z = i \frac{N_z}{L_n} \frac{\partial_X}{\sqrt{2}} E_+ \quad (11b)$$

where the subscript $_0$ has been dropped for brevity and we have changed coordinate from x to X . L_n denotes the dimensionless local density length-scale subject to the same normalization as x (Eq.5). For example, $L_n = 100$ means that it takes $100/2\pi$ vacuum wavelengths to go from the $X=0$ to the $X=1$ location.

Partial derivatives are now taken with respect to X , which allows not to make specific assumptions on the density profile $X(x)$. The magnetic field Y , on the other hand, will be treated as constant because its variation in the density gradient region is negligible in most experiments.

If the cutoffs are well separated, an O-wave starts fading at the $X=X_P$ or $X=X_L$ location (whichever is smaller) and doesn't reach the other cutoff, thus it does not couple with the X-wave. Under these circumstances, Eqs.11 reduce to separate Airy equations for E_+ and E_z , the most general solutions of which are linear combinations of Ai and Bi Airy functions. However, Bi solutions diverge and do not make physical sense here. Hence, the factor pertaining to the unphysical solution Bi has to be 0 [19]. As a result, apart from factors,

$$E_+ = Ai \left[(X - X_L) \sqrt[3]{\frac{2L_n^2}{Y+1}} \right] \quad (12a)$$

$$E_z = Ai \left[(X - X_P) \sqrt[3]{L_n^2} \right] \quad (12b)$$

These are the solutions when the O and SX cutoff are well separated. As Fig.1 illustrates, the O and SX waves evanesce exponentially after their cutoffs. Physically, this is because the polarization currents (the plasma response) grows up to complete cancelation of the displacement current $\partial \mathbf{E}/\partial t$. As a result, the O-wave is negligibly small at the other cutoff and is not capable of exciting an X-wave. This *a posteriori* legitimates having neglected the coupling terms $iN_z \partial_x / \sqrt{2}$ in Eq.11.

Note in Fig.1 that the O and SX wave domains of existence are $X < X_O$ and $X < X_{SX}$. This is consistent with their frequencies necessarily being higher than their respective cutoff frequencies, marked by arrows in Fig.2a. For optimal or about-optimal incidence, however, the dispersion relation modifies as in Fig.2b, i.e. the frequency of the mode-converted SX wave is initially smaller than cutoff, which implies access to densities $X > X_{SX}$, up to the turning point[20,2,21] $X = 1 + Y \frac{1-N_z^2}{2N_z}$.

It is intuitive that when cutoffs are only few decay-lengths far, an O wave can excite an SX wave on the other side, and viceversa. In this (general) case the coupling terms on the right hand sides of Eqs.11 have to be retained.

To eliminate E_z , we apply the operator $(X_P - X + \partial_X^2/L_n^2)$ to Eq.11a, the operator $i \frac{N_z}{L_n} \frac{\partial X}{\sqrt{2}}$ to Eq.11b and take the difference. After some algebra, we obtain:

$$\begin{aligned} & \frac{1}{2L_n^4} E_+'''' + \frac{1}{L_n^2} \left(\frac{X_L - X}{1+Y} + \frac{X_P - X}{2} + \frac{N_z^2}{2} \right) E_+'' + \\ & - \frac{2}{L_n^2} \frac{E_+'}{1+Y} + \frac{(X_P - X)(X_L - X)}{1+Y} E_+ - i \frac{N_z}{L_n} \frac{E_z}{\sqrt{2}} = 0. \end{aligned} \quad (13)$$

In the vicinity of cutoffs the partial derivatives ∂_X (proportional to iN_x) vanish at least linearly if not quadratically with X . After retaining only the zeros of lower order and taking the real part of Eq.13 while assuming, without losing generality, that E_z is real, we obtain:

$$N_z^2 \frac{1+Y}{2} E_+'' - 2E_+' + L_n^2 (1-X)(X_L - X) E_+ = 0. \quad (14)$$

In Eqs.13 and 14, the symbol ' denotes derivation with respect to X . Instead, in terms of spatial derivatives $\frac{\partial}{\partial x} = \frac{1}{L_n} \frac{\partial}{\partial X}$,

$$\frac{\partial^2 E_+}{\partial x^2} + 2\zeta N_{-,eff} \frac{\partial E_+}{\partial x} + N_{-,eff}^2 E_+ = 0 \quad (15)$$

where we have introduced

$$N_{-,eff}^2 = \frac{2}{N_z^2} \frac{(X_P - X)(X_L - X)}{1 + Y} \quad (16a)$$

$$\zeta = -\frac{\sqrt{2}}{L_n N_z} [(1 + Y)(X_P - X)(X_L - X)]^{-1/2} \quad (16b)$$

are respectively an effective squared refractive index and a damping ratio for E_+ . Note that both vary with x . The spatial non-uniformity of $N_{-,eff}^2$ implies that the wavelength changes or, when $N_{-,eff}^2$ becomes negative, it implies that the wave becomes evanescent. The non-uniformity of ζ , on the other hand, determines where E_+ decreases, and how strongly.

Unless the density gradient is extremely steep, thus L_n extremely small, the damping ratio ζ can be ignored and Eq.15 takes the form

$$\frac{\partial^2 E_+}{\partial x^2} + N_{-,eff}^2 E_+ = 0 \quad (17)$$

From Eq.16a, $N_{-,eff}^2$ can be written as $aX^2 + bX + c$, where a , b and c are constant coefficients (remember that for simplicity we are assuming uniform Y and slab geometry, thus, conserved N_z). Therefore, Eq.17 can be recognized as a parabolic cylinder equation, the solutions of which are tabulated [22,23,24].

Eq.16a can be thought of as a parabolic “potential” in X , parameterized in N_z^2 through X_L and locally representing a good approximation (Fig.3) of the Appleton-Hartree dispersion relation[18],

$$N_x^2 + N_z^2 = 1 - \frac{2X(1 - X)}{2(1 - X) - Y^2 N_x^2 / N^2 \pm \Gamma}, \quad (18a)$$

$$\Gamma = [(Y N_x / N)^4 + 4(1 - X)^2 (Y N_z / N)^2]^{1/2}. \quad (18b)$$

For $N_z^2 = N_{z,opt}^2$ (and only for that value) $X_L = X_P = 1$. Then the parabola in question develops entirely in the positive half-plane and the wave is immune from evanescent, $N_{-,eff}^2 < 0$ barriers.

This leads to the simplest solution of Eq.17, in terms of parabolic cylinder functions of order $-1/2$ [22]:

$$C = \left\{ D_{-\frac{1}{2}} \left[(-1 + i) \sqrt[4]{a}(X - 1) \right] + D_{-\frac{1}{2}} \left[(1 + i) \sqrt[4]{a}(X - 1) \right] \right\} / 2 \quad (19a)$$

$$S = \left\{ D_{-\frac{1}{2}} \left[(-1 + i) \sqrt[4]{a}(X - 1) \right] - D_{-\frac{1}{2}} \left[(1 + i) \sqrt[4]{a}(X - 1) \right] \right\} / \sqrt{2} \quad (19b)$$

where

$$a = \frac{2L_n^2}{N_z^2(1+Y)} \quad (20)$$

reduces to $a = 2L_n^2/Y$ in the present, optimal incidence case (Eq.10). The equivalent formulas

$$C = a^{1/8} \sqrt{|X-1|} J_{-\frac{1}{4}} \left[\sqrt{a}(X-1)^2/2 \right] \quad (21a)$$

$$S = \text{sign}(X-1) a^{1/8} \sqrt{|X-1|} J_{\frac{1}{4}} \left[\sqrt{a}(X-1)^2/2 \right] \quad (21b)$$

involve 1st kind Bessel functions of fractional order. These solutions, plotted in Fig.4 along with their approximations

$$C \simeq \frac{\sqrt[4]{2} \cos [\sqrt{a}(X-1)^2/2]}{[\sqrt{a}(X-1)^2 + 1]^{1/4}} \quad (22a)$$

$$S \simeq \text{sign}(X-1) \frac{\sin [\sqrt{a}(X-1)^2/2]}{a^{1/8} \sqrt{|X-1|}} \quad (22b)$$

could be termed “cosine-like” and “sine-like”, for obvious reasons. Their linear combination according to inverse prosthaphaeresis-like formulas

$$E_+ = C \sin \omega t + S \cos \omega t, \quad (23)$$

with weights determined by boundary conditions at a given instant, gives snapshots of E_+ as a function of X (or equivalently, if the density profile is linear, of x) at different times t . Here and in Fig.5 the phase is chosen to yield a sine-like E_+ at the time origin $t=0$. A tendency to longer wavelength around $X = 1$ (a reminiscence of reflectometric, Airy function behaviour) can be recognized in these graphs. Actually $\lambda \rightarrow \infty$ in that point (and only in that point). This is clear because that point is a cutoff, defined by $k_x \rightarrow 0$.

For non-optimal incidence $X_L \neq X_P$ and it is convenient to introduce the intermediate density and the semi-difference:

$$X_m = (X_L + X_P)/2 = 1 + \delta X \quad (24a)$$

$$\delta X = (X_L - X_P)/2 = -(1+Y) \Delta N_z^2/2 \quad (24b)$$

where δX is proportional to the thickness of the barrier and the systematic error in the squared refractive index, $\Delta N_z^2 = N_z^2 - N_{z,opt}^2$, is related to the systematic error in the launching angle.

For finite δX , the parabolic functions involved in Eqs.19 generalize as follows [22,23,24]:

$$E_+ = D_{-\frac{1}{2}-\frac{i}{2}\sqrt{a}(\delta X)^2} \left[(-1+i) \sqrt[4]{a}(X-1-\delta X) \right] \quad (25a)$$

$$E_+ = D_{-\frac{1}{2}+\frac{i}{2}\sqrt{a}(\delta X)^2} \left[(1+i) \sqrt[4]{a}(X-1-\delta X) \right] \quad (25b)$$

and are plotted in Fig.6. When incidence is far from optimal, Airy functions are re-obtained (Fig.6a and e). Improved launching conditions thin the evanescent barrier. The coupling terms in Eqs.11 start playing a role and each Airy function acquires an oscillatory nature beyond its respective cutoff as a result of the interaction with the other (Fig.6b and d). Optimizing N_z suppresses the barrier, maximizes the mutual influence between the O and SX solution and, thus, transmission (Fig.6c).

Transmissivity through the barrier can be defined as the ratio between the amplitudes at the barrier edges, i.e. at cutoffs, squared:

$$T = \frac{D_{-\frac{1}{2}-\frac{i}{2}\sqrt{a}(\delta X)^2}^2 [(1-i)\sqrt[4]{a}\delta X]}{D_{-\frac{1}{2}-\frac{i}{2}\sqrt{a}(\delta X)^2}^2 [(-1+i)\sqrt[4]{a}\delta X]} \quad (26)$$

This is plotted in Fig.7 and is in reasonable agreement with Mjølus formula [9],

$$T = \exp \left[-\pi L_n \sqrt{2Y} (1+Y) (N_{z,opt} - N_z)^2 \right], \quad (27)$$

here rewritten for the present geometry ($N_y=0$) and normalizations (with L_n corresponding to $k_0 L_n$ of Mjølus). In turn, this was validated against full wave calculations [16,25] and agreed within error bars with experiments [3,4,26,6]. In particular the two curves in Fig.7 exhibit the same width at half maximum. They also practically exhibit the same dependence on L_n (note the renormalized quantity on the horizontal axis), with the angular tolerance augmenting if the density gradient steepens.

In conclusion in the present Letter the problem of the mode conversion of an ordinary into an extraordinary mode has been formulated in terms of the parabolic cylinder Eq.17. Their solutions for optimal (Eqs.21) and non-optimal (Eqs.25) incidence on the cutoff layer allow to visualize the wave behavior in the vicinity of and across the degenerate cutoff (Fig.4 and 5) and evanescent barrier (Fig.6), respectively, and with realistic amplitudes, in agreement with a well-validated expression for transmissivity (Fig.7).

References

- [1] K. G. Budden, *Radio Waves in the Ionosphere*, Cambridge University Press, 1961.
- [2] J. Preinhaelter, V. Kopecký, *J. Plasma Phys.* 10 (1973) 1.
- [3] H. P. Laqua, V. Erckmann, H. J. Hartfuß, H. Laqua, W. T. ECRH Group, *Phys. Rev. Lett.* 78 (1997) 3467–3470.
- [4] H. P. Laqua, H. J. Hartfuß, W7-AS Team, *Phys. Rev. Lett.* 81 (1998) 2060–2063.
- [5] H. P. Laqua, H. Maassberg, N. B. Marushchenko, F. Volpe, A. Weller, W. Kasperek, *Phys. Rev. Lett.* 90 (2003) 75003.
- [6] F. Volpe, H. Laqua, *Rev. Sci. Instrum.* 74 (2003) 1409.
- [7] H. P. Laqua, *Plasma Phys. Controll. Fusion* 49 (2007) R1.
- [8] V. L. Ginzburg, *The Propagation of Electromagnetic Waves in Plasmas*, Pergamon Press, Oxford, 1970.
- [9] E. Mjølhus, *J. Plasma Phys.* 31 (1984) 7.
- [10] E. Tracy, A. Kaufman, A. Richardson, N. Zobin, A new normal form for multidimensional mode conversion, in: P. Ryann, D. Rasmussen (Eds.), *Radio Frequency Power in Plasmas*, 2007.
- [11] R. Cairns, C. Lashmore-Davies, *Phys. Plasmas* 7 (2000) 4126.
- [12] H. Weitzner, *Phys. Plasmas* 11 (2004) 866.
- [13] E. Gospodchikov, A. Shalashov, E. Suvorov, *Plasma Phys. Controll. Fusion* 48 (2006) 869.
- [14] A. Popov, A. Piliya, *Plasma Phys. Reports* 33 (2007) 109.
- [15] A. Popov, On o-x mode conversion in 2d inhomogeneous plasma with sheared magnetic field, arXiv.0908.1280v2 (2009).
- [16] F. R. Hansen, J. P. Lynov, C. Maroli, V. Petrillo, *J. Plasma Phys.* 39 (1988) 319–337.
- [17] Y. Podoba, H. Laqua, G. Warr, M. Schubert, M. Otte, S. Marsen, F. Wagner, *Phys. Rev. Lett.* 98 (2007) 255003.
- [18] T. H. Stix, *Plasma Waves in Plasmas*, Springer Verlag, 1992.
- [19] D. G. Swanson, *Plasma Waves*, London Academic Press, 1989.
- [20] T. Maekawa, S. Tanaka, Y. Terumichi, Y. Hamada, *Phys. Rev. Lett.* 40 (1978) 1379–1383.
- [21] H. Weitzner, D. Batchelor, *Phys. Fluids* 22 (1979) 1355–1358.

- [22] M. Abramowitz, I. Stegun, Handbook of Mathematical Functions with Formulas, Graphs and Mathematical Tables, 9th Printing, Dover, New York, 1972.
- [23] D. Zwillinger, CRC Standard Mathematical Tables and Formulae, CRC Press, Boca Raton, FL, 1995.
- [24] D. Zwillinger, Handbook of Differential Equations, 3rd Ed., Academic Press, Boston, 1997.
- [25] A. Köhn, A. Cappa, E. Holzhauer, F. Castejon, A. Fernandez, U. Stroth, Plasma Phys. Control. Fusion 50 (2008) 085018.
- [26] V. Shevchenko, G. Cunningham, A. Gurchenko, E. Gusakov, B. Lloyd, M. O'Brien, J. Preinhaelter, A. Saveliev, A. Surkov, F. Volpe, M. Walsh, Fusion Science & Technology 52 (2007) 202–215.

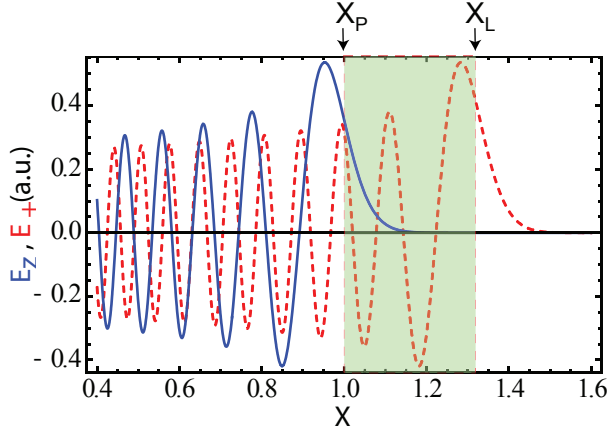


Fig. 1. O-mode (blue, solid) and X-mode (red, dashed) solutions of Eqs.11 when coupling is neglected, for $L_n=100$ and $Y=0.9$, in the vicinity of their respective cutoffs. The colored stripe represents the evanescent region in between.

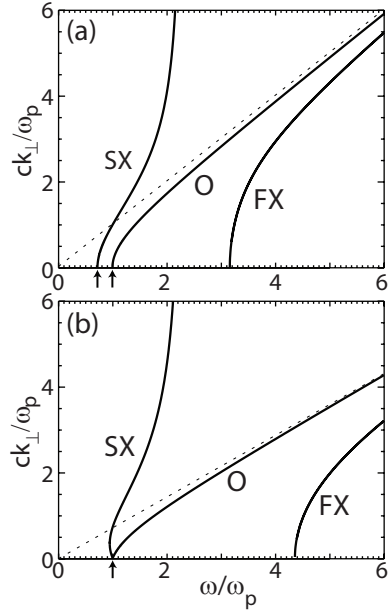


Fig. 2. Cold plasma dispersion relation of ordinary (O), fast (F) and slow (S) extraordinary (X) waves propagating (a) perpendicularly and (b) with optimal incidence with respect to a magnetic field of strength $Y=0.9$. The dashed line corresponds to propagation in vacuum, for reference. Arrows mark the distinct and degenerate, respectively, O and SX cutoffs.

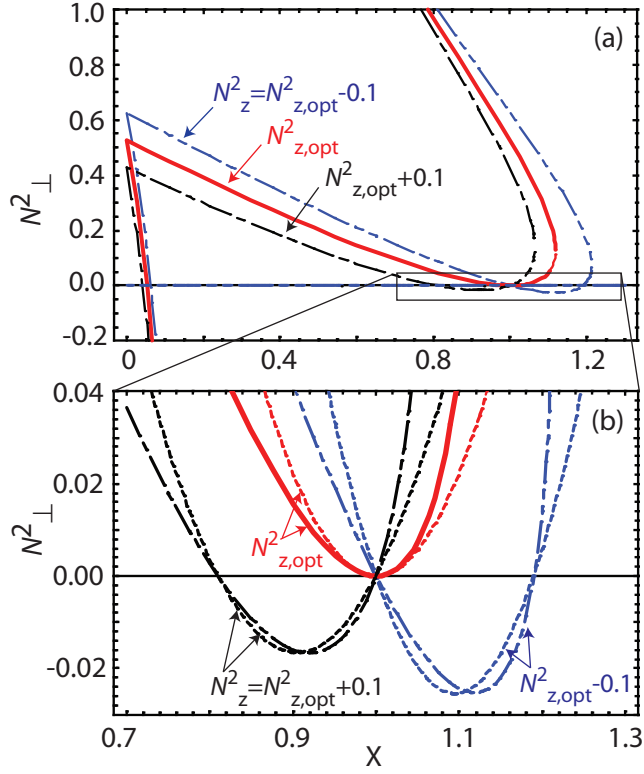


Fig. 3. (a) Appleton-Hartree dispersion relation for optimal and slightly non-optimal propagation in $Y=0.9$ and (b) comparison with Eq.16a in the vicinity of cutoffs.

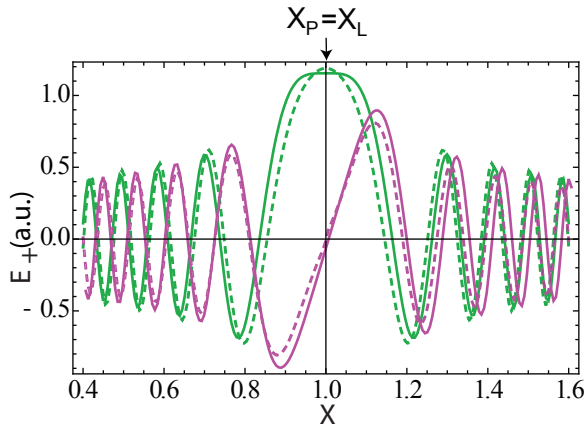


Fig. 4. Odd (purple) and even (green) exact (solid) and approximate (dashed) solutions of the parabolic cylinder Eq.17, for optimal incidence.

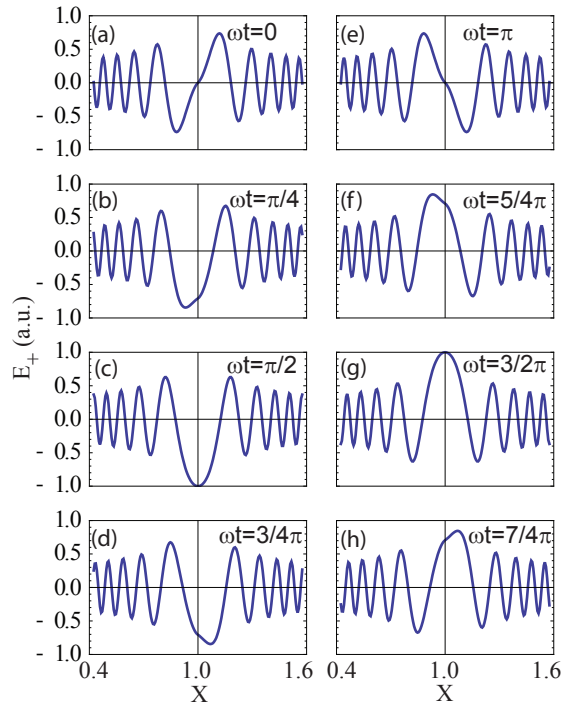


Fig. 5. Time evolution of a mode-converted O-SX wave crossing the $X=1$ cutoff with optimal incidence.

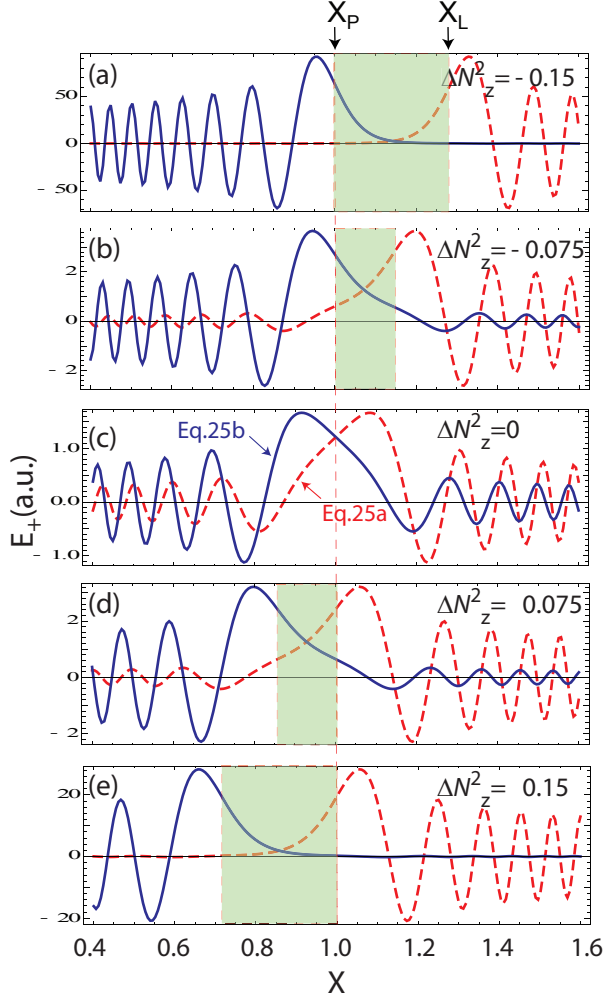


Fig. 6. Parabolic cylinder solutions, Eq.25, for values of $\Delta N_z^2 = N_z^2 - N_{z,opt}^2$ corresponding to (a) far too perpendicular, (b) slightly too perpendicular, (c) optimal, (d) slightly too shallow and (e) too shallow incidence on the evanescent barrier (green).

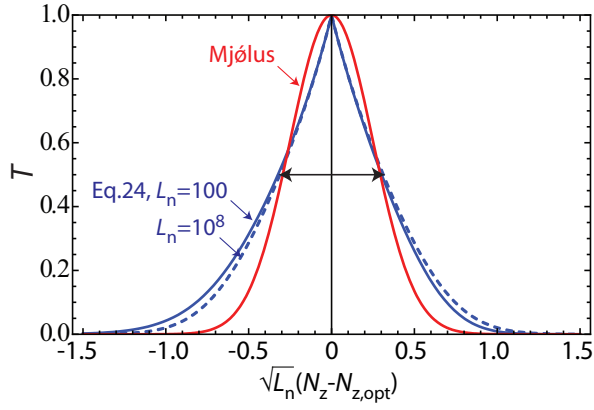


Fig. 7. Transmissivity inferred from electric field values at the barrier edges in Fig.6 (blue) and comparison with Mjølus' transmissivity (red). The latter preserves its shape, the former nearly preserves it even when the density lengthscale varies by several orders of magnitude.